

Experimental Study on the Behavior of a Swimming Pool Onboard a Large Passenger Ship

Pekka Ruponen,¹ Jerzy Matusiak,¹ Janne Luukkonen,² and Mikko Ilus³

The water in a swimming pool on the top deck of a large passenger ship can be excited to a resonant motion, even in a moderate sea state. The motion of the water in the pool is mainly caused by longitudinal acceleration, resulting from the ship's pitch and surge motions. At resonance, there can be high waves in the pool and splashing of water. In this study the behavior of the Solarium Pool of the *Freedom of the Seas* was examined in various sea states and operating conditions. The motions of the pool were calculated on the basis of a linear seakeeping method, and the behavior of the water in the pool was studied with experimental model tests. A large-scale model of the pool was constructed and fitted to a purpose-built test bench that could be axially moved by a computer-controlled hydraulic cylinder. Water elevation in the pool was measured, and all tests were video recorded. Different modifications of the pool were tested to improve the behavior of the pool. A strong correlation between the longitudinal motion and the behavior of the water in the pool was found.

Keywords: passenger vessels; ship motions; sloshing, model testing

1. Nomenclature

A = Amplitude
 g = Acceleration due to gravity
 $H(\omega)$ = Transfer function
 H_s = Significant wave height
 h = Water depth in the pool
 k = Wave number
 l = Length of the pool
 $S(\omega)$ = Spectrum
 T_1 = Mean wave period
 T_N = Natural period
 V_s = Velocity of the ship
 z_{pool} = Vertical location of the pool
 β = Angle of encounter
 δ = Phase angle
 ω = Angular frequency
 ω_e = Angular frequency of encounter

SPLASHING of water and high waves in deep swimming pools on the sun deck have taken place several times on various cruise ships during the past years, often even on a monthly basis. On many occasions, such a situation has happened in moderate waves, especially when compared with the size of the ship. If splashing takes place in the pool, it is mainly caused by the surge and pitch motions of the ship. The pools are usually located on the sun deck, high above the ship's center of gravity. Consequently, even small pitching results in large longitudinal motion of the pool. For a long and deep pool, the natural frequency of the water motion can be close to the frequency of the pitch motions. Therefore, it is possible that the water in the pool will be in resonant motion even in a normal sea state in the Caribbean.

In the early stage of design of the *Freedom of the Seas*, it was found out that the resonant motion of water in the Solarium Pool might be a problem in certain conditions. There-

fore, an extensive study on the behavior of this swimming pool was performed at Helsinki University of Technology. The investigative method and the main results of this study are presented in this paper.

2. Description of the pool

The layout of the Solarium Pool on the *Freedom of the Seas* is presented in Fig. 1, and the main dimensions of the ship and the pool are given in Table 1. The pool is relatively long and deep. There is a staircase in the aft end of the pool and wading areas with water depth of 5 cm on both sides of the pool.

The geometry of the pool is complex due to the wading areas and the staircase. Furthermore, water can be flooded to the deck if the waves in the pool are high enough. Therefore, numerical modeling of the water behavior in the pool with for instance volume of fluid (VOF) or smoothed particle hydrodynamics (SPH) is considered to be difficult and time consuming. Instead, dedicated model tests with a detailed large-scale model can provide knowledge on the behavior of the pool without resorting to complex computations.

3. Estimation of the natural period

In the case of a rectangular-shaped two-dimensional tank (see Fig. 2), the n th natural period of the water motion can be calculated from Faltinsen (1990):

$$T_{N,n} = \frac{2\pi}{\sqrt{\frac{gn\pi}{l} \tanh\left(\frac{n\pi h}{l}\right)}} \quad (1)$$

where h is the water depth and l is the length of the tank.

This formula is based on the following assumptions:

- The longitudinal cross section of the tank is rectangular.
- The walls of the tank are vertical and extend to infinity (no overflooding is allowed).
- The water depth is constant.

The assumptions of this simple formula are not valid for swimming pools on modern passenger ships since the geom-

¹ Helsinki University of Technology, Ship Laboratory, Espoo, Finland.

² Royal Caribbean International, Turku, Finland.

³ Aker Yards, Turku, Finland.

Manuscript received at SNAME headquarters February 2008.

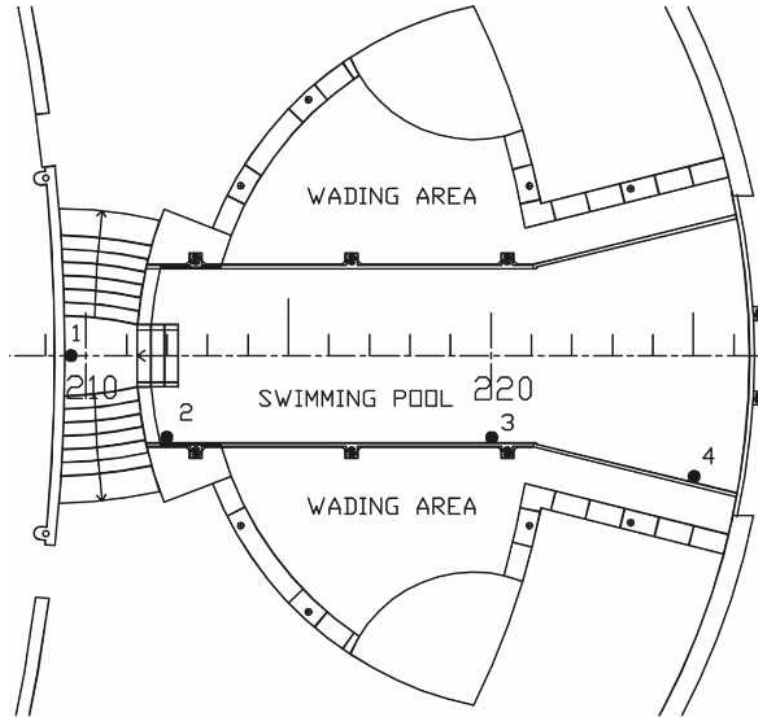


Fig. 1 Layout of the initial version of the pool and the locations of the wave height sensors (1 to 4)

Table 1 Principal dimensions of the ship and the pool

Length overall (m)	338.8
Breadth (molded at waterline) (m)	38.6
Draught (design) (m)	8.5
Depth to the upper deck (m)	47.25
Total length of the pool (m)	15.5
Breadth of the deep part of the pool (m)	4.0
Maximum depth of the pool (m)	1.95
Average depth of the pool (m)	1.55

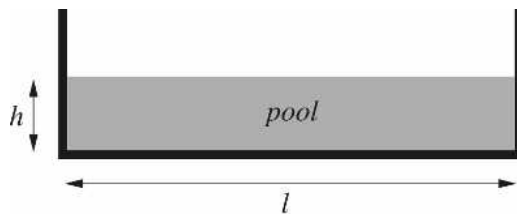


Fig. 2 Rectangular tank

etry is usually complex due to the stairs and the wading areas. Furthermore, in the studied case, also the depth of the pool is not constant.

However, this equation can be used for the first-hand estimation of the first natural period of the pool. If only the deep part of the pool (excluding the stairs) is taken into account and the average depth (1.55 m) is used, equation (1) results in $T_{N,1} = 7.0$ seconds. If the stairs are also taken into account and the water depth is taken as a little smaller (1.4 m), we get $T_{N,1} = 8.4$ seconds. If the water depth at the shallow end of the pool is used, we get $T_{N,1} = 8.7$ seconds. Therefore, the initial estimation is that the natural period is between 7 and 9 seconds. This was used as a starting point when the natural period of the pool was evaluated experimentally.

4. Motions of the pool

The longitudinal motion of the pool in various sea states was calculated theoretically by assuming that the motions of the ship in the seaway are relatively small. Hence, the effects of the other degrees-of-freedom could be ignored. It was also checked that the transverse motion of the pool is not likely to cause resonant motion of water since the natural period of the pool in the transverse direction is far from the periods of the transverse motion of the pool.

The transfer functions and phase angles for the surge and pitch motions of the ship were calculated with linear sea-keeping theory, based on Meyers et al. (1975). The underwater part of the hull was modeled in 21 sections by using 19 points in each section. The calculations were performed with different velocities and heading angles in various sea states. The applied right-handed coordinate system is presented in Fig. 3.

The longitudinal motion of the pool caused by the pitch motion θ can be estimated as the product of the pitch angle and the vertical distance between the pool and the center of gravity for the ship, z_{pool} . This is considered to be a good

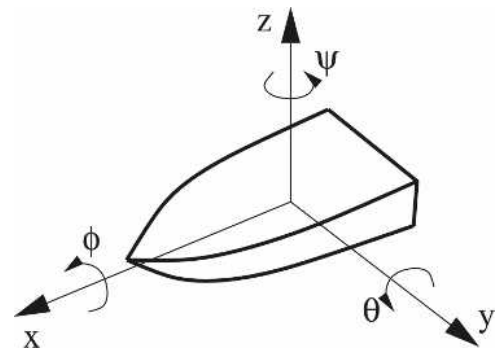


Fig. 3 Right-handed coordinate system

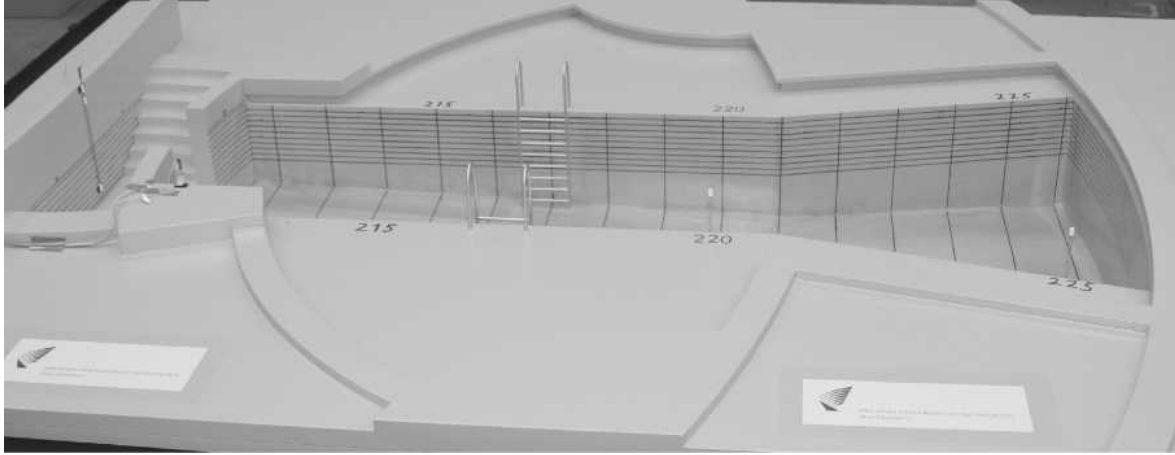


Fig. 4 The model of the swimming pool

approximation since the motions of the ship were assumed to be small.

Therefore, the transfer function for the surge motion of the pool can be written as:

$$|H_{x,pool}(\omega)| = \sqrt{[|H_{x,pool}(\omega)| \cdot \cos(\delta_{x,pool})]^2 + [|H_{x,pool}(\omega)| \cdot \sin(\delta_{x,pool})]^2} \quad (2)$$

where

$$\begin{aligned} |H_{x,pool}(\omega)| \cdot \cos(\delta_{x,pool}) &= H_x(\omega) \cdot \cos(\delta_x) \\ &\quad + k(\omega) \cdot z_{pool} \cdot H_\theta(\omega) \cdot \cos(\delta_\theta) \\ |H_{x,pool}(\omega)| \cdot \sin(\delta_{x,pool}) &= H_x(\omega) \cdot \sin(\delta_x) \\ &\quad + k(\omega) \cdot z_{pool} \cdot H_\theta(\omega) \cdot \sin(\delta_\theta) \end{aligned} \quad (3)$$

and ω is angular frequency, $H(\omega)$ is the transfer function, and δ is the phase angle for surge (x) and pitch (θ) motions.

The wave number $k(\omega)$ is defined through the dispersion relation:

$$k(\omega) \frac{\omega^2}{g} \quad (4)$$

where g is the acceleration due to gravity.

The angular frequency of encounter is:

$$\omega_e = \omega \cdot \left(1 - \frac{\omega \cdot V_s}{g} \cos\beta \right) \quad (5)$$

where V_s is the velocity of the ship and β is the angle of encounter (heading), $\beta = 180$ deg for the head seas. The corresponding period of encounter is:

$$T_e = \frac{2\pi}{\omega_e} \quad (6)$$

The spectrum of the longitudinal motion of the pool is calculated on the basis of the transfer function and the wave spectrum of the sea state $S(\omega)$, so that:

$$S_{x,pool}(\omega_e) = |H_{x,pool}(\omega_e)|^2 \cdot S(\omega_e) \quad (7)$$

The time histories for the longitudinal motion of the pool were created by using equation (7). In order to ensure that the generated time series do not comprise repeating sequences, random number generator is used to distribute discrete frequencies and to generate random phase angles of the signal components (Matusiak 2000). The amplitude of the motion is:

$$A_{x,i} = \sqrt{2 \cdot S_{x,pool}(\omega_i) \cdot \Delta\omega_i} \quad (8)$$

The spectrum for the acceleration can be calculated on the basis of the spectrum for surge motion; see e.g., Lloyd (1998):

$$S_{\ddot{x},pool}(\omega_e) = \omega_e^4 S_{x,pool}(\omega_e) \quad (9)$$

The sea states were described by the ITTC wave spectrum on the basis of the significant wave height H_s and the mean wave period T_1 .

The ITTC wave spectrum is defined as:

$$S_\omega(\omega) = \frac{A}{\omega^5} e^{B/\omega^4} \quad (10)$$

where the coefficients are:

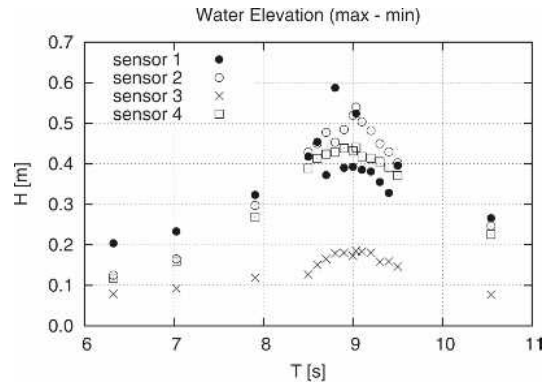


Fig. 5 Water elevations in the tests with monochromatic acceleration

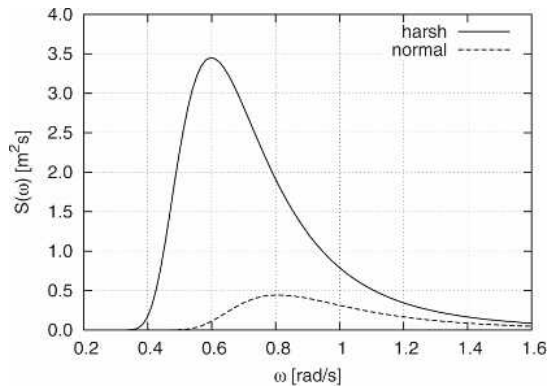


Fig. 6 Wave spectra for harsh and normal sea states

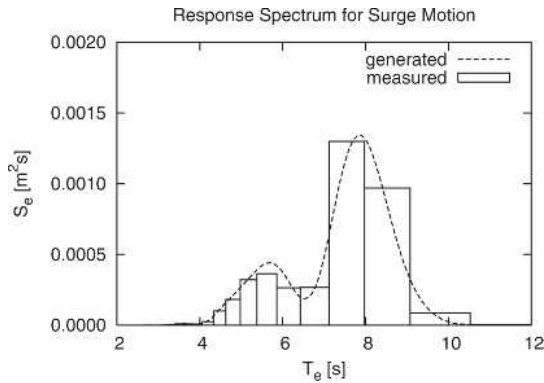


Fig. 7 Generated and measured spectra for the longitudinal motion of the pool

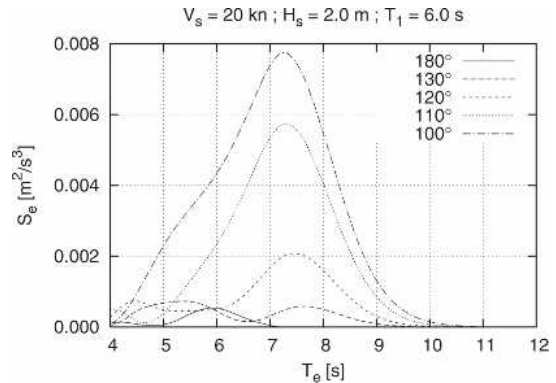


Fig. 10 Spectra for the longitudinal acceleration of the pool with various heading angles in the normal sea state

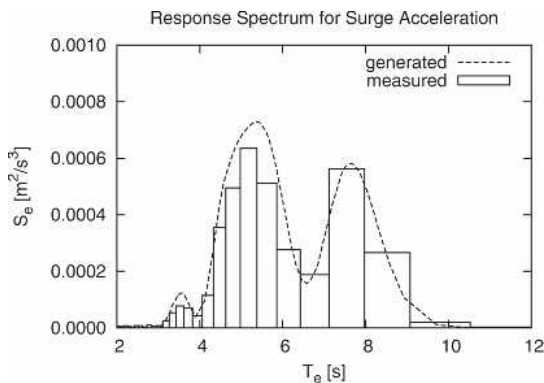


Fig. 8 Generated and measured spectra for the longitudinal acceleration of the pool

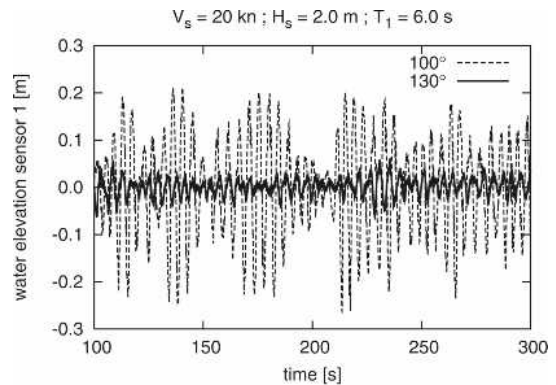


Fig. 11 Examples of the water elevations in the staircase

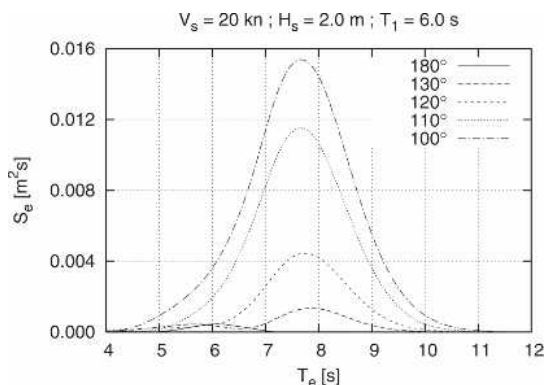


Fig. 9 Spectra for the longitudinal motion of the pool with various heading angles in the normal sea state

Table 2 Significant wave heights in the pool in normal sea state with various heading angles

β (deg)	Significant wave height in the pool (m)			
	Sensor 1	Sensor 2	Sensor 3	Sensor 4
100	0.402	0.203	0.144	0.303
120	0.185	0.140	0.057	0.128
130	0.083	0.046	0.027	0.077

Wave elevation in the pool was measured in four locations, see Fig. 1. Furthermore, the surge motion and acceleration of the pool were recorded. The volume of flooded water was calculated on the basis of the geometry and the measured decrease of the water level in the pool after the test.

$$A = \frac{173 \cdot H_s}{T_1^4} \quad (11)$$

and

$$B = \frac{691}{T_1^4} \quad (12)$$

5. Experimental setup

The model of the pool (Fig. 4) was constructed of wood on the scale 1:10. A large scale was chosen to minimize the scale effects, especially due to the surface tension in the wading areas, where the water depth in full scale is only 5 cm.

The model was installed on a purpose-built test bench that could be axially moved with a computer-controlled hydraulic cylinder. Each case was run for 10 min in model scale, corresponding to a period of 31.6 min in full scale.

6. Results

6.1. Natural period of the pool

The first natural frequency of the water motion in the pool was evaluated by performing tests with a constant amplitude and sinusoidal motion:

$$x(t) = A \cdot \sin(\omega \cdot t) \quad (13)$$

The angular frequency ω was varied. At first, tests were performed by applying a signal generator for controlling the movement of the pool. The applied frequencies in model scale were between 3 and 5 Hz with an approximate interval of 0.5 Hz. The resonance was found at the frequency of 3.5 Hz, corresponding to a period of 9.04 s in full scale. The signal generator did not allow more accurate control of the frequency. Therefore, computer control was used for full-scale

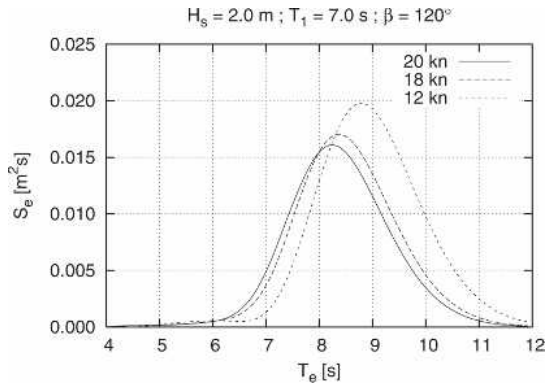


Fig. 12 Spectra for the longitudinal motion of the pool with various velocities

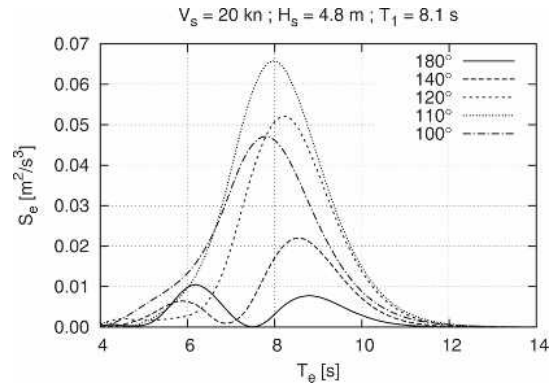


Fig. 15 Spectra for the longitudinal acceleration spectra of the pool with various heading angles in the harsh sea state

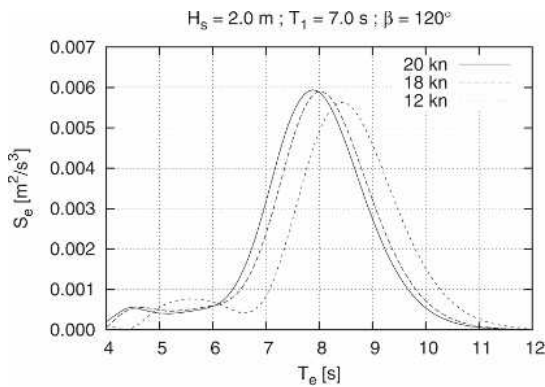


Fig. 13 Spectra for the longitudinal acceleration of the pool with various velocities

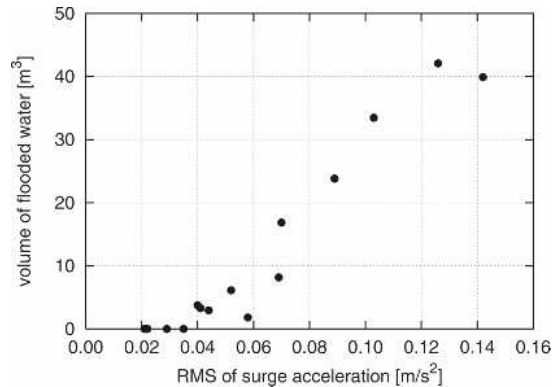


Fig. 16 Volume of flooded water as a function of the RMS value of the longitudinal acceleration in various sea states

Table 3 Volume of flooded water with various velocities during 31.6 minutes of ship operation in the normal sea state with the heading angle $\beta = 120$ deg

V_s (knots)	V_{flood} (m^3)
20	2.96
18	3.75
12	3.30

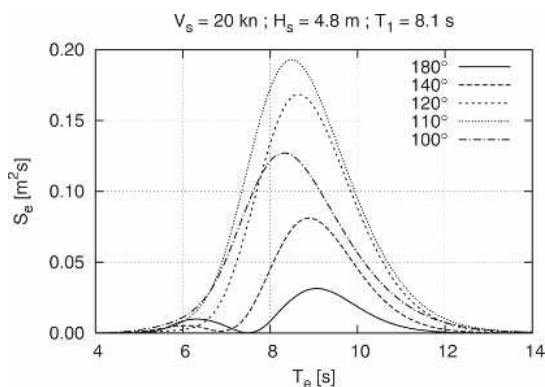


Fig. 14 Spectra for the longitudinal motion of the pool with various heading angles in the harsh sea state

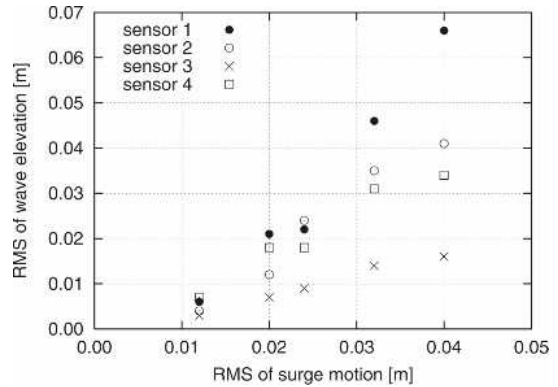


Fig. 17 RMS values of the wave elevations as a function of the RMS value of the longitudinal motion in the cases where no flooding took place

periods between 8.5 and 9.5 s with an interval of 0.1 s. Each test lasted 60 s in model scale. The applied amplitude was slightly smaller than in the initial test with the signal generator. The results for both tests are presented in Fig. 5, showing that the first natural period of the water motion in the pool is approximately 9.0 s. The sensor No. 1 was located

in the staircase. The barriers in front of the staircase and the stairs have a significant effect on the water elevation in the staircase, and therefore the results for the sensor 1 have larger variations than the other sensors.

6.2. Behavior of the pool in irregular seas

Two different sea states were selected on the basis of the research conducted by VTT (Technical Research Center of Finland) on the sea states encountered by the *Mariner of the Seas* in the Caribbean during a period of 8 months. A typical sea state has a significant wave height of approximately 2.0 m and a mean wave period of 6.0 s. This kind of sea state was encountered on a weekly basis. In the harshest sea state,

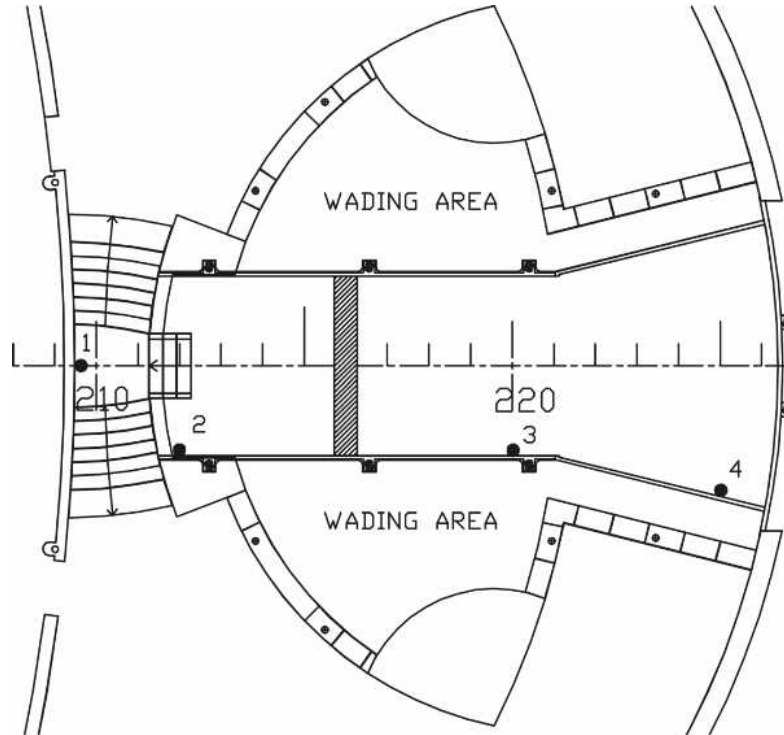


Fig. 18 Tested modification of the pool with a barrier

encountered during the analyzed period, the significant wave height was 4.8 m, and the mean wave period was 8.1 s. These two sea states, along with some variations, were used in this study. The ITTC wave spectra for the two sea states are presented in Fig. 6.

Examples of generated and measured spectra for the longitudinal motion and acceleration of the pool are presented in Figs. 7 and 8, respectively. The correspondence is good, so, apparently, the test and measurement devices worked properly.

6.2.1. Normal sea state. The response spectra for the longitudinal motion and acceleration of the pool in the normal sea state ($H_s = 2.0$ m and $T_1 = 6.0$) are presented in Figs. 9 and 10, respectively. In the head seas ($\beta = 180$ deg), the motions are insignificant, but for bow quartering seas the motions and accelerations are much larger and the peak periods are rather close to the natural period of the pool. Some examples of the measured water elevations in the staircase

(sensor 1 in Fig. 1) are presented in Fig. 11. Significant wave heights in the pool in the sensor locations are listed in Table 2 with various heading angles and constant ship velocity of 20 knots. The water elevations can be dangerously high, especially in the staircase, even in a normal sea state that is encountered on a weekly basis, if the heading angle is unfavorable.

The effect of the ship's velocity V_s on the response spectra is presented in Figs. 12 and 13. This was tested in slightly longer waves, with a mean period of 7.0 s. The effect of the velocity is rather small, only the peak period is shifted a little but the measured volume of flooded water is almost independent of ship's speed (Table 3). Therefore, at least in this particular case, the decreasing of the velocity does not improve the behavior of the pool.

6.2.2. Harsh sea state. It should be noted that in this sea state the pool would normally be closed from passengers and emptied of water. Therefore, the investigation of the behavior

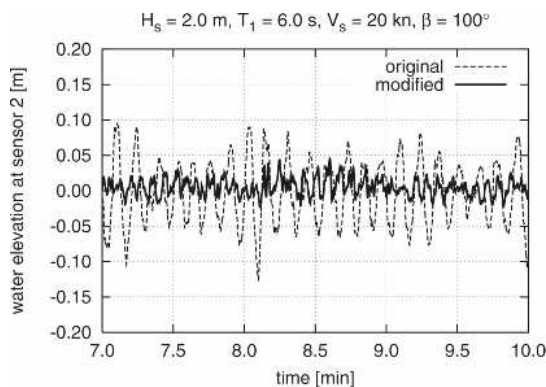


Fig. 19 Example of the wave elevations at sensor 2 for the original and modified pools in the normal sea state

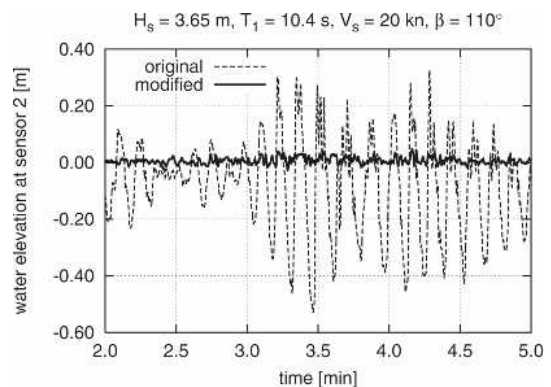


Fig. 20 Example of the wave elevations at sensor 2 for the original and modified pools in the harsh sea state



Fig. 21 The modified pool onboard the *Freedom of the Seas*

of the pool in such a sea state is purely scientific. However, the results provide useful information regarding the correlation between the behavior of the water in the pool and the motions of the pool.

The response spectra for the longitudinal motion and acceleration with various heading angles and constant velocity of 20 knots are presented in Figs. 14 and 15, respectively. The peak periods are close to the natural period of the pool. The largest motions and accelerations of the pool take place in the bow quartering as in the normal sea state. However, the motions are much larger also in general.

6.2.3. Flooded water. An almost linear correlation is found between the volume of flooded water during the test period and the root mean square (RMS) value of the longitudinal acceleration (Fig. 16). In case of small accelerations, no water is flooded, and for very large accelerations the amount of flooded water seems to be rather constant since the water level has dropped so much that no more water can be flooded anymore.

6.2.4. Water elevations. In the cases where no water was flooded, the RMS values could be evaluated for the water elevations as well. These are presented as functions of the RMS values of the longitudinal motion in Fig. 17. Obviously, larger motions of the pool cause larger wave elevations.

6.3. Effect of the modification

In order to improve the behavior of the swimming pool, several modifications were tested. The most successful, and yet simple, solution is to divide the pool into two parts with a barrier (Fig. 18).

The effectiveness of the modification was studied by performing tests with the same surge motion signal as in the case of the original layout. Some comparisons are presented in Figs. 19 and 20. The water elevations in the modified pool are much smaller than in the original version of the pool. In fact, the water elevations are not significantly high and no water is flooded, even in the harsh sea state.

On the basis of the model tests, it was decided that a dividing barrier in the pool should be installed to prevent possible problems with the resonant motion of water in the pool. However, due to architectural reasons, the barrier was placed slightly forward from the tested position, at the frame No. 221, see Fig. 21. Also, in this location the natural frequencies of the pool parts are far from the peak periods of the longitudinal motion and acceleration at the location of the pool.

7. Conclusions

The results of the study show that resonant motion of water in a long and deep pool on the top of a large passenger ship is possible even in a normal sea state that is encountered on a weekly basis. This fact should be taken into ac-

count in the early phase of the design process. The behavior of the pool can be experimentally tested on the basis of calculated time histories for the surge motion of the pool.

In this study, the natural period was evaluated experimentally. However, it was found out that the simplified approach, equation (1), provides a good first-hand estimation of the natural period of a swimming pool. If this is close to the period of pitch and surge motions, resonant motion of water in the pool is possible, and a dedicated analysis should be performed.

In the studied case, resonant motion of water in the transverse direction, mainly due to roll and sway motions of the ship, was not a problem. However, in the case of a wide pool, also this can result in resonance motion of water in some conditions.

The results of this study indicate that the transient motion of the water in the pool cannot be prevented easily with operative actions, since the heading angle should be changed significantly, and usually this is not possible. Furthermore, the velocity of the ship does not have a remarkable effect on the behavior of the pool. The only really effective method is to change the natural frequency of the pool with some structural modifications, such as the dividing barrier that was successfully tested in this study.

This research concentrated on the resonant motion of the water in the pool. However, at large heel angles water may leak over the edges of the pool to the deck, especially when the ship is turning. Also, this should be taken into account in the design and guidelines for the operation of the pools.

In the investigated pool, the wading areas were shallow, and hence a large-scale model was needed to minimize the scale effect due to the surface tension. It is believed that a smaller scale can be used if the water depth is not small anywhere in the pool.

The modified Solarium Pool has natural frequencies that are far from the peak frequency for longitudinal motion of the pool in the expected sea states and typical operating conditions. As a result, the risk of splashing in the pool is significantly reduced. In addition, there is no need to drain the pool as often as with the traditional pool layouts.

Acknowledgment

The authors would like to thank Mr. Antti Rantanen from VTT for providing the sea state statistics.

References

- FALTINSEN, O. M. 1990 *Sea Loads on Ships and Offshore Structures*, Cambridge University Press, 328 pages.
- LLOYD, A. R. J. M. 1998 *Seakeeping—Ship Behaviour in Rough Weather*, rev. ed., 395 pages.
- MATUSIAK, J. 2000 Dynamics of cargo shift onboard a ship in irregular beam waves, *International Shipbuilding Progress*, **47**, 77–93.
- MEYERS, W. G., SHERIDAN, D. J., AND SALVESEN, N. 1975 NSRDC Ship-Motion and Sea-Load Computer Program, NSRDC Report No. 3376.